A critical evaluation of topology optimization results for strut-and-tie modeling of reinforced concrete

Xia, Yi; Langelaar, Matthijs; Hendriks, Max A.N.

DOI
10.1111/mice.12537

Publication date
2020

Document Version
Final published version

Published in
Computer-Aided Civil and Infrastructure Engineering

Citation (APA)
Xia, Y., Langelaar, M., & Hendriks, M. A. N. (2020). A critical evaluation of topology optimization results for strut-and-tie modeling of reinforced concrete. *Computer-Aided Civil and Infrastructure Engineering*, *35*(8), 850-869. https://doi.org/10.1111/mice.12537

DOI: 10.1111/mice.12537

ORIGINAL ARTICLE

COMPUTER-AIDED CIVIL AND INFRASTRUCTURE ENGINEERING WILEY

A critical evaluation of topology optimization results for strut-and-tie modeling of reinforced concrete

Yi Xia[1,2] | **Matthijs Langelaar**[2] | **Max A.N. Hendriks**[1,3]

[1]Faculty of Civil Engineering & Geosciences, Delft University of Technology, Delft, Netherlands

[2]Faculty of Mechanical, Maritime and Materials Engineering, Delft University of Technology, Delft, Netherlands

[3]Department of Structural Engineering, Norwegian University of Science and Technology, Trondheim, Norway

Correspondence
Max A.N. Hendriks, Faculty of Civil Engineering & Geosciences, Delft University of Technology, Delft, Netherlands.
Email: M.A.N.Hendriks@tudelft.nl

Abstract

Defining a suitable truss model is one of the most important steps of applying the strut-and-tie modeling (STM) method to design D-regions in reinforced concrete (RC) structures. The truss model is a discrete representation of the stress field developed within a region of a concrete element. Topology optimization (TO) methods have been investigated by researchers for about two decades to generate suitable models for the STM method. Several truss models and numerous continuum TO results that could serve as an inspiration for suitable truss models have been proposed. However, limited attention has been paid to the evaluation of various TO results in the perspective of the STM method. As a result, it is at present unclear to what extent TO results offer a benefit for STM modeling, and which method should be preferred. In order to address this gap, an automatic and objective evaluation procedure is proposed in this paper. First, a TO result extraction method is proposed to systematically convert optimized topologies to truss-like structures. Next, based on the extracted structures, three evaluation measures are formulated to evaluate TO results. These measures indicate whether an analyzable truss model could be extracted, to which extent tensile stress regions are covered by tensile ties and how economical the design will be. The effectiveness of the proposed evaluation procedure is validated using known STM solutions. Subsequently, the evaluation procedure is applied to 23 TO results from the literature, covering three different design problems. Most TO results show a good performance in covering tensile regions and would result in economical designs, and some undesired topologies are also identified by the evaluation method. Nevertheless, the use of continuum TO is most hampered by difficulties in identifying a suitable truss from the TO results.

1 | INTRODUCTION

Strut-and-tie modeling (STM), a truss analogy method, is a design approach for reinforced concrete structures. The use of truss analogy models originates from 1900 (Mörsch, 1909; Ritter, 1899). In order to select a suitable model for designing concrete structures, concrete structures are subdivided into B-regions and D-regions. B-regions are the parts of a structure with linear strain distribution, where Bernoulli beam theory applies. D-regions are the remaining

parts with highly nonlinear strain distribution. Due to complex structural behavior, design codes give limited guidance to civil engineers for designing D-regions. Consequently, finding a suitable truss analogy to design D-regions is an important topic in concrete structure designs.

The STM method was further generalized as a consistent design method for different problems of reinforced concrete structures by Schlaich, Schafer, and Jennewein (1987) and Schlaich and Schafer (1991). Nowadays, it is accepted that the STM method is a practical and convenient method for designing D-regions (Karthik, Mander, & Hurlebaus, 2016; Tan, Tong, & Tang, 2001; Tjhin & Kuchma, 2007). A strut-and-tie model is created to represent the flow of stress within a concrete structure carrying loads from loading regions to supports. The STM method is based on the plasticity theory and is the result of the lower bound limit analysis (Ashour & Yang, 2008; Marti, 1985; Nielsen, 1984; Yu, Li, & Ma, 2009). Based on the lower bound limit analysis, the STM method requires a force equilibrium and satisfaction of stress constraints, while compatibility conditions are neglected. Suitable analogy models play a key role in the performance and the resulting designs are conservative. The internal forces in the truss elements are used for design or verification of concrete and (steel) reinforcements. The STM approach has been implemented in various design codes (AASHTO, 2014; ACI-318, 2008; CEB-FIB, 1993; CEN, 2017; CSA, 2004).

In various studies of STM methods, finding a suitable truss system to represent a force transfer mechanism is the first priority. In order to generate a suitable truss system for STM, the use of load path methods was suggested by Schlaich and Schafer (1991) and Mezzina, Palmisano, and Raffaele (2012). Muttoni, Ruiz, and Niketic (2015) suggested generating STM models based on the principal stress fields obtained by continuum finite element analysis. However, these methods have difficulties in generating suitable STM models for complex geometrical discontinuities and load conditions (Liang, Xie, & Steven, 2000).

Optimization techniques play a more and more important role in the structural design and industry applications. In the optimization investigations, heuristic optimization methods are powerful design tools. Adeli and Balasubramanyam (1988) applied a man-machine approach for solving the structural shape optimization. Paya, Yepes, González-Vidosa, and Hospitaler (2008) used the simulated annealing optimization method with multiple objectives to find an overall-well RC frame. Yepes, Marti, and Garcia-Segura (2015) used a hybrid glow-worm swarm algorithm to optimize precast-prestressed RC beams. The effectiveness of using genetic algorithms for structural optimizations has been investigated in a large number of studies (e.g., Aldwaik & Adeli, 2014; Kociecki & Adeli, 2014, 2015; Perera & Vique, 2009).

Topology optimization (TO) methods have been applied in designing RC structures. Bogomolny and Amir (2012) and Amir (2013) considered nonlinear material relations of concrete material in the TO process to design the steel of RC structures. TO methods have been applied by researchers to find suitable STM models as well. It is one of the most popular research directions in this field. Categorized by TO approaches, these include (i) ground structure based TO methods, (ii) ESO (evolutionary structural optimization) TO methods, (iii) density-based TO methods, for example, the SIMP (solid isotropic microstructure with penalization for intermediate densities) TO method. The relevant contributions will be discussed below. Other TO methods exist (e.g., level set methods (van Dijk, Maute, Langelaar, & Van Keulen, 2013), phase field methods (Takezawa, Nishiwaki, & Kitamura, 2010) and moving morphable components methods (Guo, Zhang, & Zhong, 2014)); however, they have not been applied for STM design yet.

Biondini, Bontempi, and Malerba (1999) and Ali and White (2000, 2001) used the ground structure based TO method to find optimized truss systems for use as strut-and-tie models. Also numerous continuum TO approaches have been explored in the past two decades. Liang et al. (2000, 2001) first used the ESO method to develop an optimized material layout for creating strut-and-tie models. Guan (2005) and Guan and Doh (2007) investigated suitable models of a deep beam under various numbers of holes and size configurations. Almeida, Simonetti, and Neto (2013) and Zhong, Wang, Deng, and Zhou (2017), Kwak and Noh (2006) considered micro-truss elements in the ESO optimization instead of continuum elements for generating optimized models. Bruggi (2009, 2010, 2016) used the SIMP TO method to generate optimized material layouts that serve as an inspiration for strut-and-tie models. The result of the SIMP TO method revealed a load path representing a force transfer mechanism of the structure. Moreover, in Victoria, Querin, and Marti (2011) and Bruggi (2016), considering the effect of different mechanical properties of steel and concrete regions, material models with different tensile and compressive moduli were used in the optimization to generate optimized models. Most researchers generated optimized topologies to use as STM models by solving the compliance optimization problem. By generating various optimized topologies for different design problems, TO methods have shown a potential to develop suitable strut-and-tie models. However, limited attention has been paid to the evaluation of these results in the perspective of the STM method. In order to fill this gap, the evaluation of continuum TO results for STM methods is our main focus.

Thus, in spite of all these studies, the question which method yields the most suitable STM model is still unanswered, and the use of TO for STM has not been widely adopted in the engineering practice. To our best knowledge, very few investigations have been carried out regarding the systematic evaluation of TO results in the perspective of the

STM method. Zhou, He, and Liu (2016) found that the current TO process was not able to directly generate desired STM models. Recently, Zhong et al. (2017) proposed a procedure to evaluate different TO results for STM models. In their method, they selected the most suitable result by visually comparing the location of ties with the tensile elastic stress field and the suspected locations of cracks, followed by an estimate of the ultimate capacity based on a nonlinear finite element analysis. Their evaluation procedure marks the first attempt to quantify the suitability of TO results for STM, but contains some manual processes and subjective choices. For example, starting with the TO result, a manual interpretation and simplification is required to obtain a truss-like structure for the STM method. Similarly, many manually adjusted STM models were found in different studies. However, variation in the manual interpretation of a TO result can considerably change the suitability and quality of the optimized result. This arbitrary topology interpretation process prevents a fair and objective evaluation of various optimized results of different TO methods. Besides, the manual interventions are impractical and inefficient for large-scale evaluations, thus an automatic method is desired.

In order to investigate to what extent TO results benefit from STM modeling and which method should be preferred, in this paper, an evaluation method is proposed to quantitatively and objectively compare the optimized topologies from different TO methods for the STM method. Note that, our aim is to perform a comparative evaluation and not to propose a new TO method. In the proposed evaluation method, manual steps to identify truss-like structures are replaced by a fully automatic truss extraction process. This process prevents and replaces ad-hoc topological changes of TO results, and may also simplify the process of using TO results for STM models by civil engineers in practice. Subsequently, an evaluation procedure including three measures is proposed to evaluate the suitability of obtained truss-like structures in the STM method. These measures indicate whether a truss model can be extracted from the TO results, to which extent tensile stress regions are covered by tensile ties and how economical the design will be. In the evaluation, the proposed indices are primarily intended for comparative evaluations. Reinforcement detailing aspects, application of minimal reinforcement ratios as required by design codes, and issues related to the constructability were not addressed explicitly in the TO studies we are evaluating. Although relevant for practical applications, these issues were consequently considered as outside the scope of our study.

In order to conduct a comparative study of various TO approaches for STM modeling, we focus on cases that have been considered in multiple studies. As these concern cases in a planar setting, our evaluation method is also defined and formulated in 2D. Nevertheless, the fundamental concepts also extend to the 3D case.

The evaluation method is implemented as an integrated and automatic procedure. Using this objective evaluation procedure, 23 TO-based results for STM modeling and 5 traditional STM models (manually generated without TO process) for three design problems are analyzed and compared based on three measures (introduced in Section 3.2). This is the first study, to our knowledge, that systematically and objectively evaluates the quality and suitability of topology optimization results for the STM method. This finally leads to recommendations for future TO research to improve its performance for generating strut-and-tie models.

This paper is organized in five parts. After this introduction section, in Section 2 our method to interpret TO results as a truss-like structure is introduced. In Section 3, the three evaluation measures are introduced and the evaluation procedure is exemplified for a simple case. Section 4 applies the truss-like structure generation algorithm and the evaluation method to three design problems which were broadly investigated in the literature. The conclusions of this paper are presented in the last section.

2 | INTERPRETING TOPOLOGY OPTIMIZATION RESULTS AS TRUSS-LIKE STRUCTURES

Strut-and-tie models are based on imaginary truss structures within the domain of the concrete volume. Strut-and-tie models based on continuum TO face the problem of interpreting TO results as a truss structure. A method that converts TO results as truss-like structures is proposed in this section.

Continuum TO results typically consist of a material distribution given by a density field, with densities ranging from 0 (void) to 1 (solid). The results are in the form of data in a matrix and do not directly provide the structural information needed for STM analysis. How to interpret TO results for further applications is another broad research field. In Hsu and Hsu (2005), TO results were interpreted by B-splines to obtain a parameterized geometry. Lin and Chao (2000) set several shape configurations to match holes of topology optimization results and then proceeded with shape optimization based on interpreted configurations. Chou and Lin (2010) and Yi, Youn, and Kim (2015) proposed methods to identify geometrical features of TO results, followed by the shape and section optimization. A similar concept was found in Yi and Kim (2017). Nana, Cuillière, and Francois (2017) proposed an automatic method to create skeletons based on TO results, and beam analysis models were created based on the pixels of the skeleton. However, none of these methods was dedicated to the extraction of STM models from continuum TO results. How to effectively extract truss-like structures based on TO results is the focus in this section.

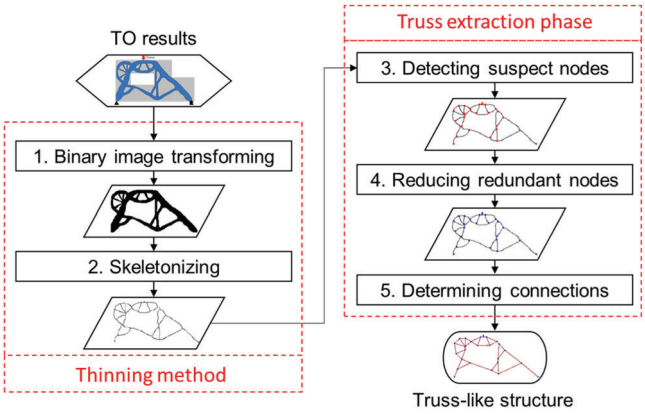

FIGURE 1 Process of the extraction method

(a) Optimized topology from Zhong et al. (2017)

(b) Coarse mesh binary image (mesh size 50, 254×120 pixels)

(c) Refined mesh binary image (mesh size 25, 508×240 pixels)

FIGURE 2 Generating binary designs based on a TO result

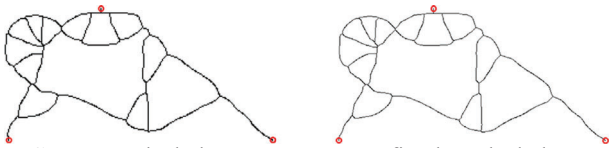

(a) Coarse mesh skeleton (mesh size 50, 254×120 pixels)

(b) Refined mesh skeleton (mesh size 25, 508×240 pixels)

FIGURE 3 Skeletons after the thinning process. The fixed load and boundary points are shown with red circles

2.1 | Process of the extraction method for optimized topologies

In the process of the extraction method for TO results, preserving a similar topology is the most important point. Mendoza-San-Agustin, Velázquez-Villegas, and ZepedaSánchez (2016) used a skeletonization method to simplify TO results without losing their topology. A similar skeletonization method is used here to provide simplified TO skeletons. Subsequently, these TO skeletons are used for identifying truss-like structures. In this paper, a truss-like structure denotes a network of straight structural members that carries forces from load points to supports. The term truss-like is coined to indicate that the network does not necessarily need to represent a suitable truss for STM analysis, as will be discussed below. In the extraction process, the nodes and their connections are identified and thus the truss-like structures are generated.

The whole process of transforming TO results to truss-like structures is shown in Figure 1. The process consists of a thinning phase, which produces the skeleton curve of the TO result. From this, nodes in the truss network are determined and connectivity information is generated, resulting in a truss-like structure. The steps of the process are described in more detail in the following subsection.

2.2 | Thinning phase

In this phase, based on image processing methods TO results are converted to simplified binary skeletons for further truss extraction. First, TO density fields are transformed to binary designs using a threshold. For our comparative study, based on the quality of TO result images from publications, an appropriate threshold is chosen in each case to capture well optimized topologies and prevent noise. For space efficiency reasons, all resulting thresholded images are not shown here but are included in Section 4.1, Figures 17–19. Next, based on the binary design, the thinning method removes the contour until the skeleton is of one-pixel width.

1. **Generating binary designs.** The optimized topologies are represented by continuous density fields. For further processing, first clear solid/void (0/1) binary designs based on TO density fields are generated. A TO result by Zhong et al. (2017) is used as an example. In this case, the grayscale image of the optimized topology is the source data. The binary design is obtained by setting the threshold at 0.5 to determine the 1-bit number of a pixel. The obtained binary designs of different resolutions are shown in Figure 2. Figure 2b is the result of a coarse mesh case, and Figure 2c is the result of a refined mesh.
2. **Thinning.** Image skeletons are simplified data containing the topology information and can be extracted from the source binary data through the thinning process. Skeletonization methods have been widely investigated. Huang et al. (2013) extracted the skeleton curve from a point cloud. Jiang, Xu, Cheng, Martin, and Dang (2013) used graph contraction to obtain a curve skeleton. Abu-Ain, Abdullah, Bataineh, Abu-Ain, and Omar (2013) applied a thinning method to extract the skeleton.

In this paper, the thinning method from Zhang and Suen (1984) is used to skeletonize TO results. Its basic working principle is an iterative removal of boundary pixels, until the skeleton curve remains and no further pixels can be removed without changing the topology. In this method, pixel-wise elimination rules are first set. Next the method detects the local binary images with pixel dimension 3×3 and the binary image is thinned iteratively. For further details, the reader is referred to Zhang and Suen (1984). The generated skeletons are shown in Figure 3. The load and boundary points are taken as fixed black pixels which remain present during the

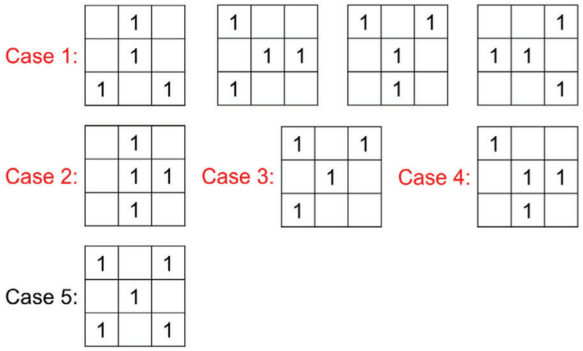

FIGURE 4 Set of patterns used for determining candidate nodes

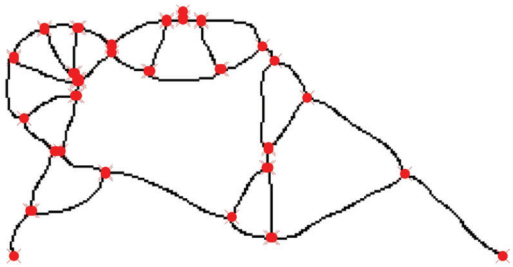

FIGURE 5 The skeleton after identifying candidate nodes, indicated in red

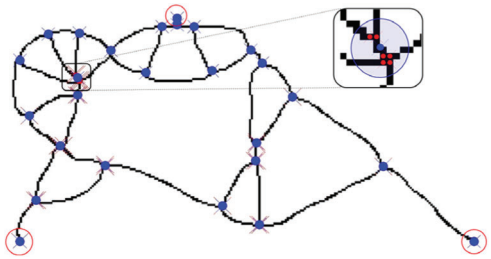

FIGURE 6 The example with reduced nodes, indicated in blue. The tolerance area to reduce redundant nodes is presented with blue regions in the enlarged inset. The nodes marked by a red circle are not connected to any hole

thinning process. As long as the topology can be maintained, the computational time of the topology interpretation process is reduced by reducing pixels. For efficiency, a relatively coarse mesh size is used in this paper. The obtained skeletons provide the essential information to identify truss-like structures.

2.3 | Truss extraction phase

In order to create truss-like structures, based on the topology skeleton the procedure of identifying nodes and bars is proposed in this section. The detailed steps of the truss extraction method in Figure 1 are presented below:

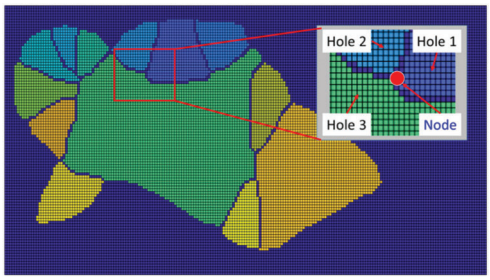

FIGURE 7 Identification of holes and topology relation of a node

3. **Detecting candidate nodes.** The obtained skeleton is stored as a binary image. Whether a pixel in the skeleton is denoted as a candidate node is based on its value and the values of the eight neighboring pixels. Figure 4 shows all five cases where a pixel is identified as a node. Note that the cases 1 to 4 include four rotationally equivalent cases, as is shown for case 1 only. If the pixel pattern of the skeleton matches one of these cases, it is selected as a candidate node. The candidate nodes of the skeleton from Figure 3b are marked in Figure 5.
4. **Reducing redundant nodes.** Several candidate nodes may cluster in a small region. A reduction method is used to reduce redundant candidate nodes. If the mutual distance of candidate nodes is smaller than a preset tolerance (5% of the length of the shortest edge of the original domain), then this set of nodes is replaced by a single node at the averaged location. The reduced nodes of the example are shown in Figure 6.
5. **Determining connections.** After determining the nodes, their connections are required to obtain truss-like structures. First, the holes of the skeleton are identified. The identification process is similar to the process in Lin and Chao (2000). All nonskeleton pixels are detected sequentially and pixels adjacent to each other and surrounded by skeleton pixels are marked as a hole, shown in Figure 7.

   The hole information of nearby nodes is stored as topology information. For each node, it is determined which holes of the node is adjacent to. Based on the center point of each hole and the vertical direction, the nodes are ordered clockwise around the hole and connected by lines, shown in Figure 8. Some nodes may not be connected to any hole, such as load points and support points (Figure 6). These nodes are connected to a nearby node, starting from connecting to the closest node and checking the match of the connected line to the skeleton. Although this method may potentially fail with certain pathological shapes, it has proven effective for all TO results tested in this study. The resulting truss-like structure of this case is shown in Figure 9.

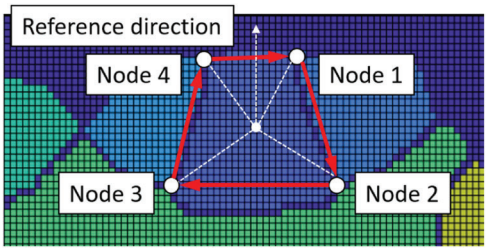

FIGURE 8 Determining connections for a hole. The connections are indicated by red arrows

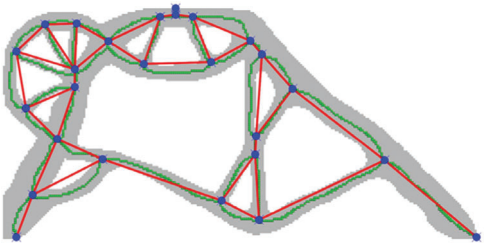

FIGURE 9 Obtained truss-like structure. The grey part is the binary TO result, the green pixels form the thinned skeleton, blue points and red lines are the identified nodes and members, respectively

3 | EVALUATION PROGRESS OF TOPOLOGY OPTIMIZATION RESULTS

In this section, three main measures are defined to evaluate the obtained truss-like structures for their suitability in the STM method. The first measure is the STS (Suitable Truss Structure) index. It measures the degree to which the obtained truss-like structure, as identified from the TO result, can be analyzed and forms an axial-force equilibrium system that is suited for the STM method. Note that STM models are often kinematic; however, any slight change of the model geometry would induce diagonal compression forces in the concrete to stabilize the structure (El-Metwally & Chen, 2017). The second measure is the TRS (tensile region similarity) index. It measures whether the tension regions in optimized topologies spatially correspond to the regions of tensile stress in the original full domain. Covering tensile stress regions in original concrete domain is considered as an advantageous property of the truss analogy as the resulting steel layout will limit severe concrete cracking before reaching the ultimate loading capacity of the D-region (FIB, 2011). The third measure is the SR (steel reinforcement) ratio. It provides an estimate of how much reinforcement steel will be required for the proposed truss analogy and it thus indicates how economical the design will be.

3.1 | Framework of the evaluation method

An automatic evaluation method is proposed. The framework is shown in Figure 10. At the beginning of the evaluation process, images of TO results are used as input files. In this paper, we use 21 different TO results and 5 traditional STM models for three design problems from the literature. Two more TO results are created using SIMP TO method to provide a more complete comparison and discussion. These results will be introduced in Section 4.1. Based on the TO result extracting method from the previous section, a set of truss-like structures can be extracted for a certain design problem. The process provides a uniform platform to compare various TO results from the literature for the same design problem. Next, finite element analysis (FEA) is used to obtain the structural response. The four-node bilinear quadrilateral element under the plane stress assumption is used for the continuum full concrete domain and the classical beam element is used for the truss-like structure. Use of beam elements is necessitated because the truss-like structures generated by the truss extraction process are usually statically and kinematically unstable trusses. The equilibrium forces of unstable structures cannot be calculated through truss analysis. Based on the obtained structural response, the STS index and SR ratio are calculated. However, determining the TRS index needs two more steps introduced in the following section. After calculating these three measures, the advantages and disadvantages of various TO results for STM can be evaluated.

3.2 | Evaluation measure definition

3.2.1 | Suitable truss structure (STS) index

In the STM method, a basic requirement is that all members are subjected to an axial-force equilibrium state. However, we find that the truss-like structures generated by the truss extraction process often do not meet this requirement. For our comparative evaluation, it is relevant to quantify the closeness of the structure to an analyzable truss. In order to discuss this point, slender beam elements are used to analyze the interpreted truss-like structures. The slender beam model has members with a low bending stiffness. The axial forces are obtained for conventional kinematic STM models. The shear forces indicate (unwanted) moments in the elements. In the slender beam element analysis, the cross section is assumed as rectangular in which the width equals to the out-of-plane thickness of the original continuum and the height is 1% of its width. The distribution of axial and shear forces stabilizes as slenderness is increased, hence this thickness is chosen as an adequate value. The resulting axial forces and shear forces are used to formulate the STS index, defined in Equation (1):

$$\mathrm{STS} = \frac{1}{n} \sum \frac{|N_e|}{|N_e| + |V_e|} \tag{1}$$

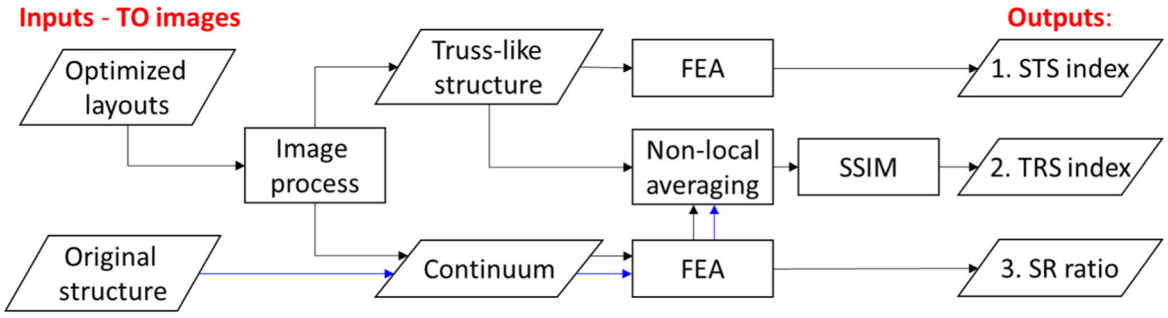

FIGURE 10 Framework of the evaluation method

where N_e is the element axial force, V_e is the element shear force, and n is the number of elements. The STS index has the range [0, 1]. When STS = 1, all members in the truss-like structure are subjected to axial forces only and it can be used as-is in the STM method. For lower values, adjustments would be necessary before use in the STM method, however these modifications are outside our scope. In this study, our focus is on comparing suitability of the results provided by TO methods. Results with a lower STS index are further from true truss structures, and therefore less desired.

3.2.2 | Tensile region similarity (TRS) index

Tensile stress is critical to concrete structures. Following recommendations by Schlaich and Schafer (1991) and Bergmeister, Breen, Jirsa, and Kreger (1993), Schlaich et al. (1987), the position and orientation of ties and struts should ideally reflect the stress field of a linear analysis of the complete domain. This will prevent excessive cracking at the service load level (whereas the STM method is a capacity check at the higher ultimate load level). Considering that steel reinforcements are located and aligned at the places where they contribute most to the bearing capacity of the structure (for the ultimate limit state) and avoid excessive concrete cracking (for the serviceability limit state), it is especially relevant that the tensile regions of the stress fields are well covered by ties of the truss. Therefore, tensile stress fields of the original structure and TO results are compared to formulate the TRS index. Based on linear FEA, the principal stress vectors $\boldsymbol{\sigma}^{\mathrm{ori}}$ and $\boldsymbol{\sigma}^{\mathrm{TO}}$ of the original structure and optimized results are obtained, where σ_{I} and σ_{II} are first and second principal stress respectively ($\sigma_{\mathrm{I}} > \sigma_{\mathrm{II}}$). In this paper, the critical tensile regions are defined as those, where the first principal stress is much larger than the second principal stress, $\sigma_{\mathrm{I}} > 0$ and $\sigma_{\mathrm{I}} > -5\sigma_{\mathrm{II}}$. Based on the tensile stress, the TRS index is formulated after a nonlocal averaging operation and image comparison, as defined below.

Two important aspects must be included in formulating the TRS index. First, a larger volume fraction in the TO process leads to topologies with wider structural members. Regardless of the volume fraction, TRS indices should be similar as long as the main topology is comparable. Second, the reinforcement would improve the crack-resisting capacity of the nearby concrete. So, the criterion has been formulated such that it is relatively insensitive to changes in volume fraction and to minor differences in positioning of tensile regions/members. The nonlocal averaging operation is used to determine the influenced tensile region. This operation has been applied in the investigation of fracture behavior analysis (see Bažant & Jirásek, 2002), the sensitivity filtering in TO methods to solve mesh-independence and checker-board problems (see Sigmund & Petersson, 1998), and achieving the minimum length scale in the TO process (see Guest, Prévost, & Belytschko, 2004). In this paper, the stress of tensile regions is spread through nonlocal averaging. The nonlocal averaging is implemented through the filter, defined as:

$$\overline{\boldsymbol{\sigma}}_i = \frac{\sum_{j=1}^{n} h(i,j) \cdot \boldsymbol{\sigma}_j}{\sum_{j=1}^{n} h(i,j)} \tag{2}$$

where $h(i, j)$ is a convolution filter, $\boldsymbol{\sigma}_j$ is the stress of element j whereas $\boldsymbol{\sigma}_j = \mathbf{0}$ outside the tensile region, $\overline{\boldsymbol{\sigma}}_i$ is the averaged stress of element i which is affected by surrounded elements. The stress vectors $\boldsymbol{\sigma} = \{\sigma_x, \sigma_y, \tau_{xy}\}$ of all elements in the tensile region are filtered. Next, the averaged principal stresses are calculated based on the averaged stress $\overline{\boldsymbol{\sigma}}$. The convolution filter $h(i, j)$ is defined as:

$$h(i,j) = \max(0, r_0 - r(i,j)) \tag{3}$$

where $r(i, j)$ indicates the centroid distance between elements i and j, and r_0 is the averaging radius, defined as:

$$r_0 = \frac{1}{2}\frac{V}{L \cdot t} \tag{4}$$

Here, V is the volume of the original structure, L is the total length of the extracted truss-like structure calculated by summing lengths of all its members, and t is the thickness of the original structure. Based on this formulation, as long as the main topologies of different optimized results are the same, the extracted truss-like structures are the same and their total length L is also equal. Therefore, the radius is the same for these results regardless of the volume fraction and minor topology differences.

After obtaining the averaged tensile stress fields, the TRS index quantifies the similarity of two stress fields with the help of an image analysis method. The image analysis method quantifies the difference of images compared to a reference image. The SSIM (structural similarity) index for image comparison was proposed in Wang, Bovik, Sheikh, and Simoncelli (2004). It quantifies the similarity between two samples based on three metrics: luminance, contrast, and structure (C. Li & Bovik, 2010; Wang et al., 2004). The calculation of the SSIM index is defined as:

$$\mathrm{SSIM}(\boldsymbol{a},\boldsymbol{b}) = \frac{[2\mu(\boldsymbol{a})\mu(\boldsymbol{b})+C_1][2\tau(\boldsymbol{a},\boldsymbol{b})+C_2]}{[\mu^2(\boldsymbol{a})+\mu^2(\boldsymbol{b})+C_1][\lambda^2(\boldsymbol{a})+\lambda^2(\boldsymbol{b})+C_2]} \tag{5}$$

where $\boldsymbol{a}$ and $\boldsymbol{b}$ are two sample data, μ is the sample mean, λ is sample standard deviation, and τ is the sample correlation coefficient. C_1 and C_2 are chosen as 10^{-6} to avoid a zero in the denominator. The SSIM index has the range [0, 1], where 0 means extremely poor similarity and 1 means perfect similarity.

In this paper, the SSIM analysis is used to compare stress fields. First, the averaged tensile principal stress of the original structure and optimized results are scaled as $\hat{\boldsymbol{\sigma}}^{\mathrm{ori}}$ and $\hat{\boldsymbol{\sigma}}^{\mathrm{TO}}$ respectively, where $\hat{\boldsymbol{\sigma}} = \overline{\boldsymbol{\sigma}}_{\mathrm{I}}/\max(\overline{\boldsymbol{\sigma}}_{\mathrm{I}})$ is the averaged first principal stress in the tensile region. Next, the SSIM index is used to quantify the similarity between the tensile principal stress field in the topology optimized structure and the original structure, which defines the Tensile Region Similarity or TRS index, defined as:

$$\mathrm{TRS} = \mathrm{SSIM}(\hat{\boldsymbol{\sigma}}^{\mathrm{ori}}, \hat{\boldsymbol{\sigma}}^{\mathrm{TO}}) \tag{6}$$

A larger TRS index indicates that the topology optimization result is effective in representing the tensile regions of the original structure.

3.2.3 | Steel reinforcement (SR) ratio

The amount of steel usage is an important aspect in designing RC structures. Efficient steel utilization results in a less costly design. In this paper, the steel reinforcement ratio is taken as the third metric to compare various TO results. Based on the FEA structural response of the TO results, the SR ratio is calculated as the volume fraction of steel with respect to the concrete volume, defined as:

$$\mathrm{SR} = \frac{1}{V_{\mathrm{ori}}} \int \frac{\max(\sigma_{\mathrm{I}}, 0)}{f_y} \mathrm{d}\Omega_e \tag{7}$$

In the equation, f_y is the yield strength, Ω_e denotes the elements in the tensile region, and V_{ori} is the total volume of the original structure. The proportions of the positive first principal stress to the yield strength indicate the usage of steel in designing RC structures. Throughout the paper $f_y = 450\,\mathrm{MPa}$ has been assumed.

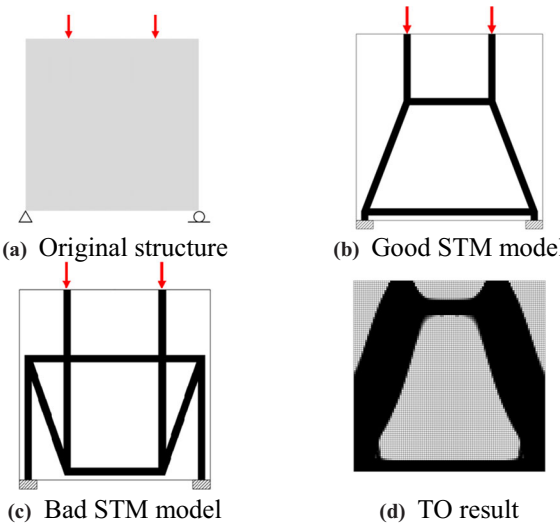

FIGURE 11 Geometries considered to illustrate the evaluation method. (a) Shows the deep beam design problem; (b) and (c) show manually generated STM models; (d) shows the TO result

3.3 | A simple case for illustration

A classical case study is used to illustrate the evaluation method. The basic information of the case is shown in Figure 11. In the figure, (a) shows load and boundary conditions of the deep beam of equal length and height (2 m). The thickness of the structure is 0.1 m, the concentrated forces are 1000 kN, Young's modulus is 30 GPa, Poisson's ratio is 0.2, and the yield strength is 450 MPa. Figure 11b and c are the relatively good and bad strut-and-tie models provided by Schlaich and Schafer (1991), where all members have been given a thickness of 0.1 m, and the designs are represented by images that can be processed by our evaluation method in the same way as TO results, and Figure 11d is our example TO result based on compliance minimization using the SIMP method (Andreassen, Clausen, Schevenels, Lazarov, & Sigmund, 2011). The optimized topology is obtained with 50% volume fraction of the original structure and using the sensitivity filtering technique (Sigmund & Petersson, 1998).

Following the proposed evaluation method from Figure 10, Figure 12 depicts the result of truss extraction applied to each of the topologies. After FEA of the continuum, the principal stress plots are shown in Figure 13.

Based on the obtained truss-like structure, the total lengths of all members of three truss-like structures are 6.92 m, 9.92 m, and 6.85 m, respectively, and the radius r_0 in the nonlocal averaging analysis is 0.29 m, 0.2 m, and 0.29 m. The averaging domains are shown in Figure 12. Figure 14 shows the scaled averaged tensile principal stress after nonlocal averaging, using a grayscale color scheme. The TRS indices are subsequently calculated through SSIM analysis. The evaluation results are shown in Table 1. Comparing results of two STM models by Schlaich and Schafer (1991), a bad

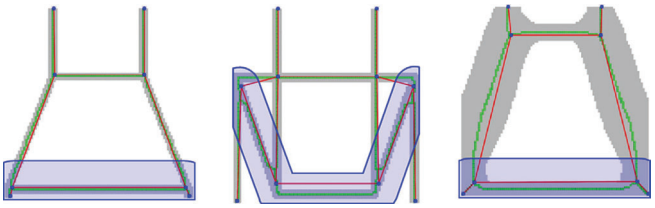

(a) Good STM model (b) Bad STM model (c) TO result

FIGURE 12 Results after image processing and truss extraction. The blue regions indicate the averaging domains in the nonlocal averaging operation

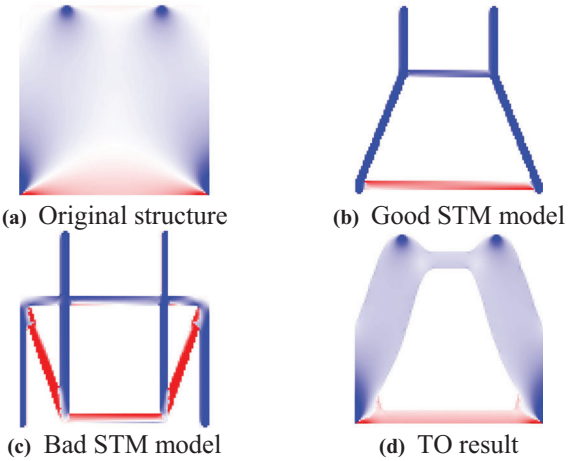

(a) Original structure (b) Good STM model (c) Bad STM model (d) TO result

FIGURE 13 Principal stress plots. Red and blue parts indicate the tensile and compressive regions, respectively

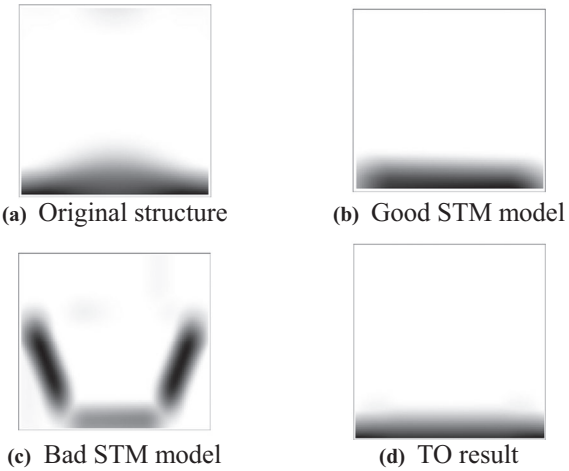

(a) Original structure (b) Good STM model (c) Bad STM model (d) TO result

FIGURE 14 Scaled tensile principal stress after nonlocal averaging

TABLE 1 Evaluation results of the illustrative case study, worst scores are presented in bold (%)

Cases	STS index	TRS index	SR ratio
Good STM model	98.8	83.7	1.59
Bad STM model	99.3	**46.4**	**4.82**
Optimized result	**93.6**	84.1	1.42

model in the STM method results in a higher SR ratio and a lower TRS index. The evaluation result based on the optimized topology has a higher TRS index and a lower SR ratio than the two strut-and-tie models. However, the extracted truss-like structure has a lower STS index, i.e., more shear force than the other two cases, which indicates it is not a pure truss structure. This is primarily due to the orientation of the bars near the load and support points. An adaptation toward a proper truss structure is possible, but the lower STS index is indicative of the fact that some modification is needed.

4 | STM CASE STUDIES FROM THE LITERATURE

4.1 | Problem introduction

Based on different considerations and requirements in the perspective of the STM method, researchers have proposed different TO methods to generate a large variety of optimized layouts, as reviewed in the first section. The majority of papers have explored multiple 2D problems and proposed several optimization results. A limited number of papers (Almeida et al., 2013; Guan and Doh, 2007; Zhong et al., 2017; Zhou et al., 2016) also contained strut-and-tie models; however, these models were not directly determined from the optimized topology and usually manual changes were made. Regardless of various applications of different TO methods, efforts were proposed to improve the TO method, such as, smoothing the constitutive relation in the optimization process, considering different tensile and compressive moduli, and using microstructure based elements instead of continuum elements. We found three cases which were investigated relatively frequently: a deep beam with square opening, a corbel, and a dapped-end beam with rectangular opening (Figure 15). These cases form the basis for our comparison of TO-based STM models. Various published results are evaluated, compared, and discussed in this section.

In the evaluation process, the thickness of the structures is 300 mm, the Young's modulus and Poisson's ratio are 20 GPa and 0.2, respectively. The principal stress plots of the full concrete domains are plotted in Figure 16, where red and blue regions show the tensile and compressive regions, respectively.

Table 2 gives an overview of the considered topology results from the literature that are used in this section. In order to shorten the length of the paper, the detailed settings of all these results are shown in Table A1 in the Appendix. The study includes 28 different results from 11 individual papers. The TO results of the three cases, as extracted from the publications at identical resolution, are shown in Figures 17, 18, and 19. The test set contains a variety of models that allow comparisons of different aspects. Results I-10 and I-11

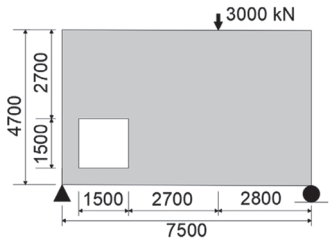

(a) Case I: Deep beam with opening

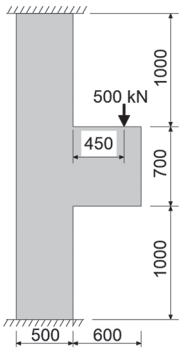

(b) Case II: Corbel

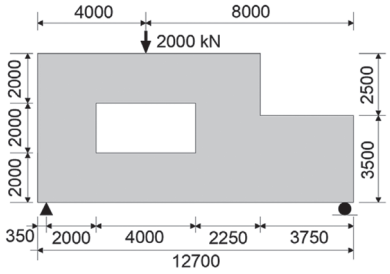

(c) Cass III: Dapped-end beam with opening

FIGURE 15 Basic information of three cases (mm)

(a) Case I: Deep beam with opening (mesh size: 50mm)

(b) Case II: Corbel (mesh size: 10mm)

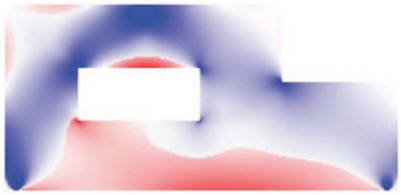

(c) Case III: Dapped-end beam with opening (mesh size: 50mm)

FIGURE 16 Principal stress plots of three cases. Red and blue parts indicate the tensile and compressive regions, respectively

are generated by a conventional SIMP optimization method with a 40% volume fraction and sensitivity filtering. The traditional STM models which were proposed without using TO methods are recreated as continua in our study (Results I-1, I-2, II-1, III-1, and III-2). Results I-3 and II-2 are generated based on a conventional ESO method by Liang et al., 2000).

TABLE 2 Categorization of TO results of three cases

Literature	Result I	Result II	Result III
Schlaich et al. (1987)	I-1,2	II-1	–
Liang et al. (2000)	I-3	II-2	–
Kwak and Noh (2006)	I-4,5	II-3,4	–
Bruggi (2009)	–	II-5,6	–
Reineck (2002)	–	–	III-1,2
Victoria et al. (2011)	I-6,7,8	II-7,8	–
Herranz, Maria, Gutierrez, and Riddell (2012)	–	–	III-3
Gaynor et al. (2013)	–	–	III-4,5
Almeida et al. (2013)	I-9	II-9,10	–
Zhou et al. (2016)	–	–	III-6
Du et al. (2019)	–	II-11	–
This paper	I-10,11	–	–

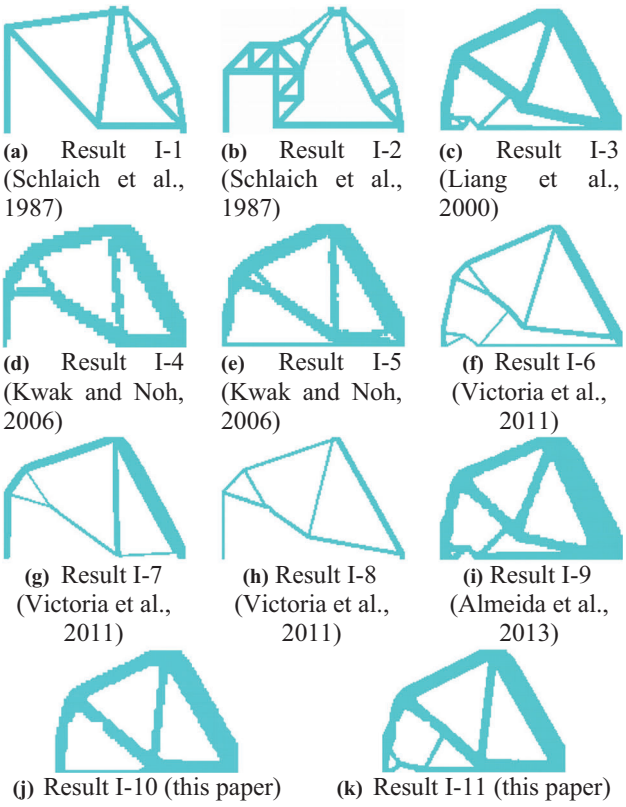

(a) Result I-1 (Schlaich et al., 1987)
(b) Result I-2 (Schlaich et al., 1987)
(c) Result I-3 (Liang et al., 2000)
(d) Result I-4 (Kwak and Noh, 2006)
(e) Result I-5 (Kwak and Noh, 2006)
(f) Result I-6 (Victoria et al., 2011)
(g) Result I-7 (Victoria et al., 2011)
(h) Result I-8 (Victoria et al., 2011)
(i) Result I-9 (Almeida et al., 2013)
(j) Result I-10 (this paper)
(k) Result I-11 (this paper)

FIGURE 17 Case I: Topology optimized results of the deep beam with an opening

The mesh size is an aspect affecting TO results. Optimized results with coarse mesh sizes are shown as Results I-4, I-10, II-3, II-5, and II-9. In contrast, Results I-5, I-11, II-4, II-6, and II-10 are optimized topologies for corresponding cases using a refined mesh size. Victoria et al. (2011) considered different tensile and compressive moduli in the optimization process: Results I-7 and II-8 are optimized topologies with a larger tensile modulus, while Results I-6 and II-7 are commonly

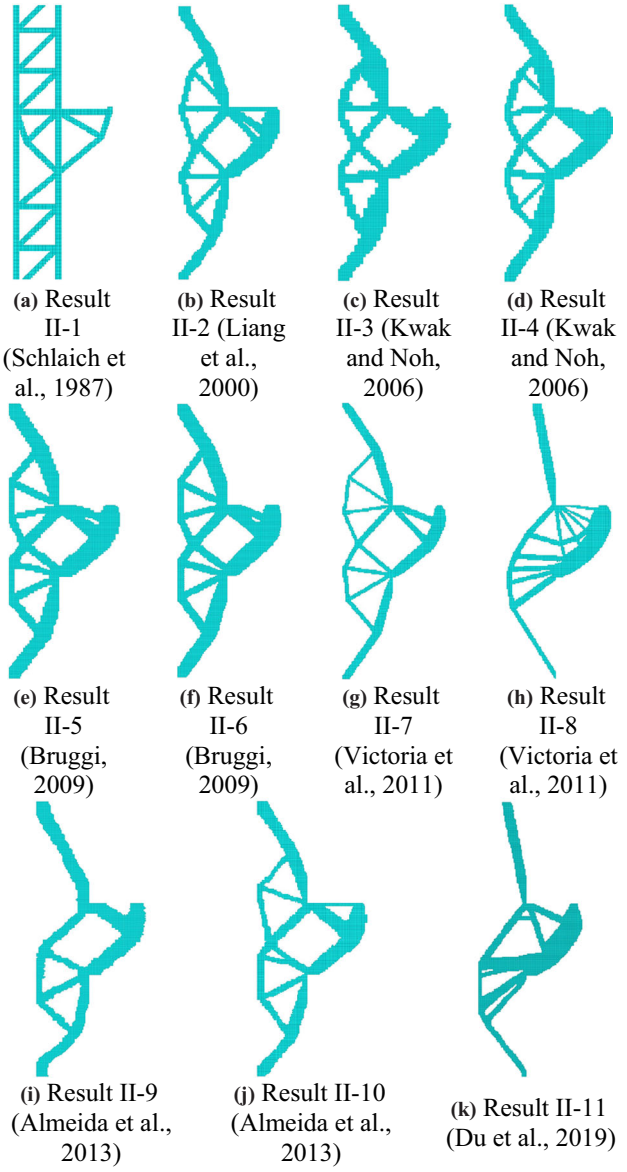

(a) Result II-1 (Schlaich et al., 1987) (b) Result II-2 (Liang et al., 2000) (c) Result II-3 (Kwak and Noh, 2006) (d) Result II-4 (Kwak and Noh, 2006)

(e) Result II-5 (Bruggi, 2009) (f) Result II-6 (Bruggi, 2009) (g) Result II-7 (Victoria et al., 2011) (h) Result II-8 (Victoria et al., 2011)

(i) Result II-9 (Almeida et al., 2013) (j) Result II-10 (Almeida et al., 2013) (k) Result II-11 (Du et al., 2019)

FIGURE 18 Case II: Corbel

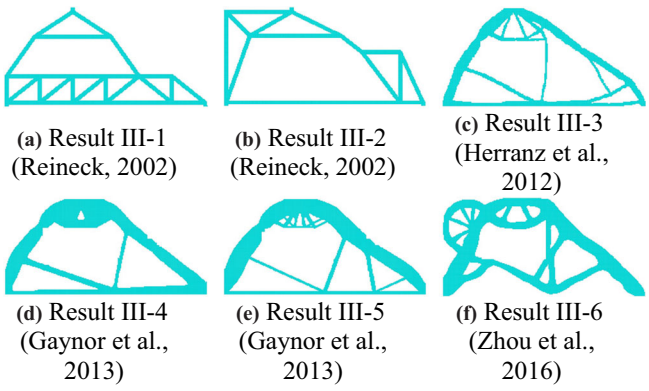

(a) Result III-1 (Reineck, 2002) (b) Result III-2 (Reineck, 2002) (c) Result III-3 (Herranz et al., 2012)

(d) Result III-4 (Gaynor et al., 2013) (e) Result III-5 (Gaynor et al., 2013) (f) Result III-6 (Zhou et al., 2016)

FIGURE 19 Case III: Dapped-end beam with opening

TABLE 3 Evaluation results for Case I: Deep beam with an opening, best and worst scores are presented in bold (%)

Results	STS index	TRS index	SR ratio
I-1	94.8	**61.5**	0.861
I-2	**96.8**	66.3	**1.111**
I-3	**77.0**	81.0	0.761
I-4	94.1	64.9	0.894
I-5	93.9	78.0	0.744
I-6	95.7	72.1	0.80
I-7	94.4	65.2	0.978
I-8	95.1	64.1	0.928
I-9	77.5	**83.0**	**0.717**
I-10	92.8	77.8	**0.717**
I-11	88.9	81.4	**0.717**
Avg	91.0	72.3	0.839
Std	7.09	8.13	0.129

optimized topologies with the same method. Moreover, the topology using a small volume fraction is shown as Result I-8. Similarly, Du, Zhang, Zhang, Xue, and Guo (2019) proposed an orthotropic material model considering different tensile/compressive modulus in the SIMP TO process. Result II-11 is the optimized result obtained by using a large tensile modulus. A truss-continuum hybrid topology optimization method was proposed in Gaynor, Guest, and Moen (2013), the optimized result and a reference result based on conventional TO are included as Results III-5 and III-4, respectively. Result III-3 is generated by using the full-homogeneous optimization method. Result III-6 is generated by using the ESO method with the removal criterion of the first principal stress.

Using the 3-measure evaluation process defined in Section 3, all considered models have been evaluated. Section 4.2 presents the results, followed by further discussion in Section 4.3.

4.2 | Evaluation results of three cases

Here, the results of the three cases are discussed individually. Overall result analysis and discussion are provided in Section 4.3. The evaluation result of Case I is shown in Table 3, the principal stress plots for this case are shown in Figure 20, the extracted truss-like structures are shown in Figure 21. The considered traditional strut-and-tie models (that are not based on TO), have a relatively high STS index. Indeed, they are designed as trusses. They have a relatively low TRS index since they miss a tensile tie bottom-left, below the opening. The models based on TO score higher on average for representing the tensile region, with exceptions (Results I-4,7,8). Among the different TO results, Result I-9 has the highest TRS index. Also on average, optimized models have

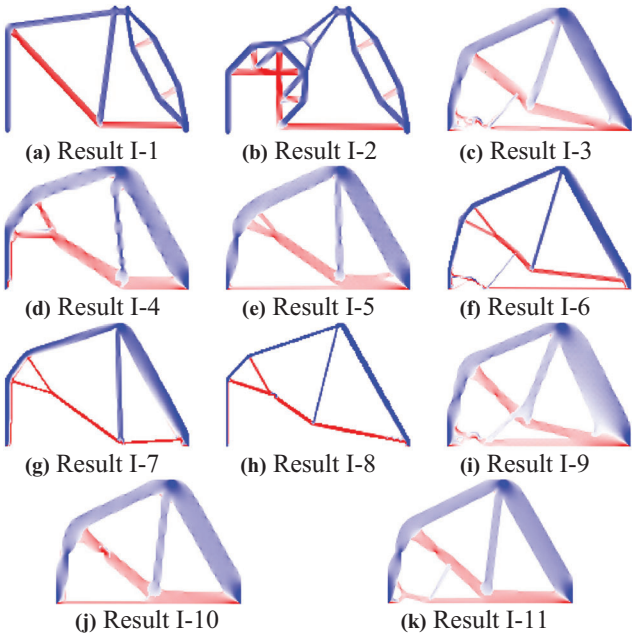

FIGURE 20 Principal stress plots of Case I: Deep beam with an opening. Red and blue parts indicate the tensile and compressive regions, respectively

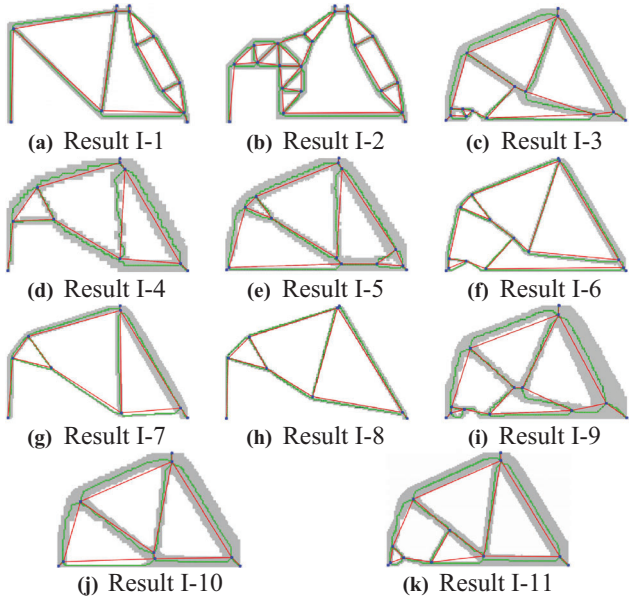

FIGURE 21 Extraction results of Case I: Deep beam with an opening

small SR ratios, which indicates less steel utilization. The lowest SR ratios are obtained in Results I-9, I-10, and I-11, while again Results I-4, I-7, and I-8 score comparatively worse. Traditional STM models result in larger SR ratios than TO-based models. Overall, the TO-based models of Results I-5, I-10, and I-11 show good performance. On the contrary, Results I-4, I-7, and I-8 show a relatively poor performance.

TABLE 4 Evaluation results for Case II: Corbel, best and worst scores are presented in bold (%)

Results	STS index	TRS index	SR ratio
II-1	**98.5**	**72.7**	1.53
II-2	92.1	75.3	1.36
II-3	93.9	76.9	**1.26**
II-4	**91.1**	**77.5**	1.28
II-5	93.4	76.3	1.30
II-6	93.8	76.4	1.28
II-7	98.4	75.4	1.36
II-8	94.6	74.6	**2.69**
II-9	92.0	73.1	1.54
II-10	93.5	76.0	1.39
II-11	93.6	73.1	2.54
Avg	94.1	75.2	1.59
Std	2.38	1.64	0.515

TABLE 5 Evaluation results for Case III: Dapped-end beam with an opening, best and worst scores are presented in bold (%)

Results	STS index	TRS index	SR ratio
III-1	**97.8**	69.7	0.917
III-2	95.3	55.9	**1.01**
III-3	91.6	70.7	**0.539**
III-4	89.5	**71.3**	0.550
III-5	96.2	69.4	0.561
III-6	**71.1**	**50.7**	0.928
Avg	90.3	64.6	0.751
Std	9.87	8.94	0.222

In order to shorten the length of the paper, the principal stress plots and recognized results for Case II and Case III are shown in the Appendix. The evaluation result for Case II is shown in Table 4. From the standard deviation of indices, it is seen that this case has an overall stable result, except for Result II-8 and Result II-11 which have considerably larger SR ratios than the other results. All results have an overall high STS index. In general, the traditional STM model again has a slightly smaller TRS index and larger SR ratio than topology optimized results. In this case, Results II-8 and II-11 would require more than twice the amount of steel compared to the most economical design.

The evaluation results of Case III are shown in Table 5. Similar to the previous two cases, traditional STM models show smaller TRS indices and larger SR ratios. The topology optimized results show similar performance with the exception of Result III-6, which performs poorly on all three aspects.

Based on the evaluation results of three cases, Case II is less sensitive to TO methods than the other cases. Most of the TO results lead to similar results even when the optimized

topologies are different visually. No matter what type of TO approach (ESO, SIMP, full-homogeneous method, etc.) is used, in general, topology optimized results have better scores in representing the tensile region of the original structure and will result in less steel utilization than traditional STM models. However, the recognized truss-like structures of the TO results have less than ideal STS indices, which indicates that the results cannot be directly applied in the STM method.

4.3 | Discussions of results

In this section, based on the evaluation results of three cases, four main aspects are analyzed and discussed. Firstly, the influence of using different material models in the TO process on the three suitability measures is discussed. Secondly, the optimization result is usually a local minimum based on a certain set of parameters in the TO process. Similarly, the influence of different optimization parameters is discussed. Thirdly, the advantages of using TO methods are discussed by comparing them to conventional STM models. Lastly, regarding the axial-force equilibrium requirement for the STM, the suitability of the generated truss-like structures based on the proposed extraction method is discussed.

4.3.1 | Influence of different material models in the topology optimization

In the literature related to the use of TO for STM modeling, methods have been proposed to obtain better results. Instead of using isotropic continua, different material models (in broad sense) in the TO method have been proposed in the literature. Based on the evaluated cases, three aspects are discussed in this section: (a) using micro-truss elements instead of continuum elements, (b) considering different tensile/compressive moduli, (c) using truss-continuum hybrid elements.

Firstly, instead of plane stress elements, micro-truss elements were used in the optimization procedure. The results are included as Result I-4 & 5, Result II-3 & 4, and Result III-6. Kwak and Noh (2006) demonstrated that the optimization results using micro-truss elements were less sensitive to mesh size and more efficient in finding strut-and-tie models than classical ESO methods. The absence of the tensile members at the bottom of Result I-4 is the key reason for the observed performance reduction. Comparing the evaluation of Result I-3 with Result I-5 and Result II-2 with Result II-4 regarding the TRS index and the SR ratio (see Tables 3 and 4), no obvious improvements are observed using micro-truss elements. However, in Case I the force equilibrium system is significantly closer to an axial-force equilibrium using micro-truss elements.

Secondly, optimization procedures involving different tensile and compressive moduli were considered in Victoria et al. (2011) and Du et al. (2019). These studies aimed to include the effect of the different mechanical properties of steel and concrete regions, in order to obtain better STM layouts. The optimized results of these cases are clearly different from the results using the isotropic material model. The optimized results considering the orthotropic tensile/compressive material model are shown in Results I-7, II-8, and II-11. Based on the evaluation results, these optimized results lead to high SR ratios and low TRS indices in both Case I and Case II, and are surpassed by cases using standard linear elastic material models.

Thirdly, Gaynor et al. (2013) used a truss-continuum hybrid element and considered an orthotropic material model during the optimization procedure, as shown in Result III-5. In this way, the truss elements in the hybrid model provide orthotropic mechanical behavior in the tensile regions, which has a similar effect as using different tensile and compressive moduli in a continuum model. The optimized result in this case leads to a high SR ratio and a low TRS index, which is similar to the results obtained from the orthotropic material model.

Generally, we have not observed a case where more sophisticated material models or discretizations resulted in a clear benefit in terms of quality of the resulting STM models. In the evaluated cases considering bi-modulus material properties, due to tensile material having a larger stiffness, the topology optimization process results in designs that contain more tensile material. In the studied examples, better results were obtained using standard linear elastic material models. This is a counter-intuitive result, as generally more sophisticated modeling should lead to more efficient designs. As an example, nonlinear finite element analysis to study crack patterns provides much more detailed design information than a linear elastostatic analysis. An investigation towards more effective ways to include refined material behavior in the TO process for STM models, actually leading to noticeable improvements, is recommended as future research.

4.3.2 | Influence of different settings in the topology optimization method

The optimized result in the TO process is a local minimum of different solutions to the same design problem when choosing different parameters in the TO method (Sigmund & Petersson, 1998). In this section, the parameters affecting TO results in different TO methods thus affecting the suitability of results to be used as STM models are discussed based on the evaluated cases. These parameters include: (a) removal criteria in ESO methods, (b) mesh sizes of the analysis model, (c) TO volume fraction, and (d) different TO methods.

Firstly, the influence of the removal criteria in ESO methods is discussed. Liang et al. (2000) and Kwak and Noh (2006) used the strain energy removal criterion in the

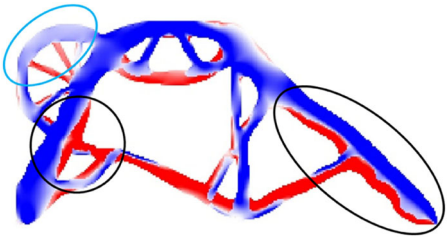

FIGURE 22 Principal stress plot of Result III-6. Red and blue parts indicate the tensile and compressive regions, respectively

ESO method, whereas Almeida et al. (2013) took the Von Mises stress removal criterion and smoothed the material constitutive relation in the optimization process. Similarly, the Von Mises stress removal criterion was used in Victoria et al. (2011). Comparing their result (I-6) with Result I-3 of the ESO method based on the strain energy criterion, the topology optimized layouts are similar. Consequently, the evaluation results of these cases are similar as well. This observation is confirmed by the earlier study by Q.Q. Li, Steven, and Xie (2006), who demonstrated the equivalence of using the Von Mises stress criterion and the strain energy criterion in the ESO method.

In the study by Zhou et al. (2016), the first principal stress was taken as the removal criterion in the ESO method. Result III-6 is the optimized layout which is determined as a suitable optimization result based on their evaluation procedure. However, by comparing the evaluation result with others (see Table 5), Result III-6 results in the lowest TRS index and a relative large SR ratio, thus it may not be a good choice to create STM models. In order to analyze the lower performance of this case, its principal stress plot is shown in Figure 22. In the figure, severe bending behavior is observed in the region within black circles, which leads to the low TRS index and indicates that this layout is far from a truss model, and thus leading to a low STS index as well. The region within the blue circle was introduced by the authors to cover the tension in the original structure, shown in Figure 16c. However, from our analyses the indicated arch is in compression (Figure 22), and does not contribute to a better TRS index.

Secondly, the influence of mesh size of the analysis model is discussed. In Case I, regarding the TRS index and SR ratio, Result I-5 based on the ESO method with the refined mesh size performs better than Result I-4 with the coarse mesh size. However, based on TO results generated by the SIMP method, by comparing the evaluation results of coarse mesh size results (I-10 and II-5) with refined mesh size results (I-11 and II-6), only small differences are observed. In fact, the filter technique in the SIMP method prevents the mesh dependency problem. Similarly this filter technique can be applied in ESO methods to improve results (Huang & Xie, 2010).

Thirdly, the volume fraction affects the numbers of members and their width in the optimized results. In Result I-6 and Result I-8, different volume fractions for one TO method are used. With a much lower volume fraction in the optimization, Result I-8 has a lower TRS index and a larger SR ratio than Result I-6. A similar observation applies to Result II-9 and Result II-10. Regarding to the three measures Result II-10 with a relatively large volume fraction performs better than Result II-9. However, with a small volume fraction in the optimization, generally a relatively simple optimized topology is obtained. This is beneficial for extracting truss-like structures resulting in a high STS index.

Fourthly, we compare different types of TO methods for STM. In the SIMP TO method, the optimized results are generated by solving the compliance optimization problem. They are very comparable to results of ESO methods with the strain energy or Von Mises stress removal criterion. This can be observed by comparing evaluation results of classical ESO methods with the SIMP method in Case I and Case II. They have similar TRS indices and SR ratios. Similar conclusions are observed by comparing the Isoline method and the full-homogeneous method with the ESO method (SIMP method). Generally, regarding the TRS index and the SR ratio, these methods have similar performance, although their optimized results show some differences. All of these results perform well in representing tensile regions and leading to economical designs.

4.3.3 | Comparing TO results to conventional strut-and-tie models

Finding a unique and suitable model for the STM is one of the most important reasons to use objective-oriented TO methods. Based on the evaluation results of the considered cases, this aspect is discussed in this section.

Results I-1,2, II-1, and III-1,2 are the conventional STM models. In Case I, regarding to the TRS index, Result I-1 performs better than Result I-2, however the comparison of SR ratios leads to the opposite result. In Case III, Result III-2 performs better than Result III-1 for both the TRS index and the SR ratio. It is difficult to manually improve the conventional STM models. Based on the previous discussion on different TO methods in the fourth part in Section 4.3.2, the evaluation of TO results only shows slight differences for the same problem. Moreover, TO results have better performance in the TRS indices and the SR ratios comparing to conventional STM models in all three cases. Although it should be noted that an evaluation of compression struts was outside the scope of our measures, these observations confirm the prospects of using TO methods to find suitable STM models.

4.3.4 | The axial-force equilibrium requirement

Most of the studied TO methods could provide helpful layouts as inspiration for generating suitable STM models.

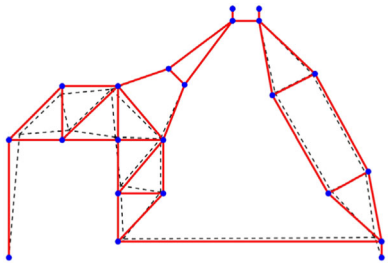

FIGURE 23 Truss-like structure of Result I-2. Dashed lines indicate the generated truss-like structures and solid lines show the adjusted structure

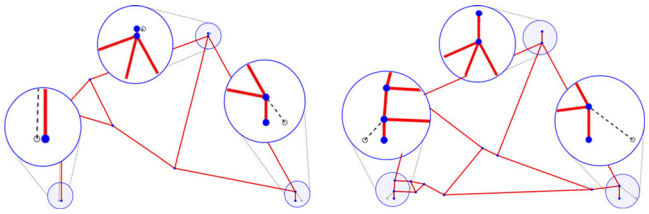

(a) Result I-8 (b) Result I-3

FIGURE 24 Truss-like structure with zoomed-in details. Dashed lines indicate the generated truss-like structures and solid lines show the adjusted structure

However, none of them can be applied in the STM method directly without further manual post-processing. The STM method requires an axial-force equilibrium system. As long as the generated truss-like structures have STS indices less than 1, shear force is present. The shear forces can be resisted by the surrounding concrete, however in this way, this model cannot fully represent the stress mechanism for the structure, thus they cannot be used as an STM model. This problem can originate from the provided topology, and the truss extraction process in Section 2 also affects the suitability of truss-like structures. The node positions can be shifted due to the thinning and node clustering in the extraction process. An example is shown in Figure 23. In the figure, the model with dashed lines shows the truss-like structures generated through the extraction process. The solid-line model indicates the adjusted truss model in which the positions of nodes are manually adjusted to a geometry similar to the conventional STM model, aligning members with applied loads and reaction forces. The three indices (STS, TRS, SR) of the two truss-like structures are (96.8%, 66.3%, 1.11%) and (99.8%, 66.5%, 1.11%), respectively. An improvement of the STS index is noted, as expected. Little change is seen in the other indices of the two truss-like structures. The truss-like structure based on the traditional STM model provides an axial-force equilibrium system and can be used in the STM method.

In some cases, by similar manual adjustments, the STS indices of truss-like structures based on the TO results can be improved. An example of Result I-8 is shown in Figure 24a, three indices (STS, TRS, SR) are (95.1%, 64.1%, 0.928%) and (99.8%, 64.1%, 0.928%), respectively. Especially, the STS index is improved from 95.1% to 99.8%, which is close to a desired axial-force equilibrium state. However, this manual adjustment does not work for all cases: an example of Result I-3 shows insufficient improvement of the STS indices from 77.0% to 92.8% (Figure 24b), while TRS and SR indices again remain similar.

5 | CONCLUSIONS

In this paper, an automatic and objective evaluation method is proposed to evaluate TO results generated by various methods for use in strut-and-tie modeling, in order to enable a comparison between the many approaches suggested for this problem. In the evaluation procedures, a dedicated topology interpretation method is proposed to create truss-like structures from optimized layouts. In this way, the topology results can be processed and evaluated in an automatic and systematic manner. Next, based on the analyzed structural response, three measures are proposed for comparing various topology optimized layouts in the perspective of strut-and-tie modeling. The STS index measures the degree to which truss models based on the TO results can be analyzed and form an axial-force equilibrium system that is suited for the STM method. The TRS index measures the effectiveness of TO results in representing tensile regions of the original structures. The SR ratio indicates how economic the design will be. Together, these criteria form our definition of suitability of a TO result for the purpose of STM modeling. In total 28 results of three design problems are evaluated and discussed. Based on the present investigation, the conclusions are summarized as follows:

1. The proposed evaluation method can reliably deal with a wide variety of cases automatically. The method provides an objective way to evaluate various optimized layouts, without manual intervention. The method has been presented here for planar cases, but the concept extends naturally to 3D. Implementation of a thinning method for voxel images and connectivity detection for 3D skeletons would be required. Moreover, in order to evaluate the practical structural performance of STM models, such as crack behavior and failure mode, nonlinear finite element analysis can provide additional insight.
2. Many efforts were investigated by researchers to improve topology optimization methods to generate better layouts for the STM method. Based on our present evaluations, we do not observe an obvious improvement of nonstandard TO methods or more sophisticated material models over conventional approaches. These efforts may not be the most important steps towards improving the suitability

of TO for the STM method. Interestingly, by considering a large tensile stiffness in the tension/compression orthotropic material model, the TO process results in more tensile regions. This clearly leads to worse STM results in the studied cases compared to simple isotropic material assumptions, and indicates potential for improved formulations in which results do benefit from refined material modeling.

3. Different parameters and settings in the TO process that affect optimized layouts have been investigated, such as the mesh size, removal criteria in ESO methods, volume fractions, and different types of TO methods. Based on the analyzed cases, the filtering technique is suggested to solve the mesh dependent problem in the TO process. The strain energy and the Von Mises stress removal criteria in the ESO methods result in the similar results. However, the result based on the first principal stress criterion leads to a poor performance. All the applied TO (ESO, SIMP, Isoline and Full-homogeneous) methods generally have similar and good performance for the STM.
4. Comparing with conventional STM models, most topology optimization results perform better in representing the key tensile regions and limiting steel usage. Topology optimization methods are therefore promising and powerful tools to provide information for the STM method.
5. Currently, without manual adjustment, continuum TO procedures typically do not result in truss structures. The truss structure extraction method is proposed in this paper to solve this problem. However the resulting truss-like structures may be not in a pure axial-force equilibrium state. In other words, in contrast to the expectations found in many papers on this topic, the generated TO-based layouts are not directly suitable for the STM method. Generating truss structures in the TO process that fully satisfy the STM requirements is identified as an open problem in this field.

ACKNOWLEDGMENTS

The authors would like to thank professor Yue Wu (Harbin Institute of Technology) for useful suggestions. The authors would like to thank the Editor and the anonymous reviewers for their constructive comments and valuable suggestions to improve the quality of the article.

REFERENCES

AASHTO. (2014). *LRFD bridge design specifications* (7th ed.). Washington, DC.: Author.

Abu-Ain, W., Abdullah, S. N. H. S., Bataineh, B., Abu-Ain, T., & Omar, K. (2013). Skeletonization algorithm for binary images. *Procedia Technology*, *11*, 704–709.

ACI Committee 318. (2008). *Building code requirements for structural concrete and commentary*. Farmington Hills, MI: American Concrete Institute.

Adeli, H., & Balasubramanyam, K. (1988). A synergic man-machine approach to shape optimization of structures. *Computers and Structures*, *30*(3), 553–561.

Aldwaik, M., & Adeli, H. (2014). Advances in optimization of highrise building structures. *Structural and Multidisciplinary Optimization*, *50*(6), 899–919.

Ali, M. A., & White, R. N. (2000). Formulation of optimal strut-and-tie models in design of reinforced concrete structures. *ACI Special Publication*, *193*, 979–998.

Ali, M. A., & White, R. N. (2001). Automatic generation of truss model for optimal design of reinforced concrete structures. *Structural Journal*, *98*, 431–442.

Almeida, V. S., Simonetti, H. L., & Neto, L. O. (2013). Comparative analysis of strut-and-tie models using smooth evolutionary structural optimization. *Engineering Structures*, *56*, 1665–1675.

Amir, O. (2013). A topology optimization procedure for reinforced concrete structures. *Computers and Structures*, *114–115*, 46–58.

Andreassen, E., Clausen, A., Schevenels, M., Lazarov, B. S., & Sigmund, O. (2011). Efficient topology optimization in Matlab using 88 lines of code. *Structural and Multidisciplinary Optimization*, *43*(1), 1–16.

Ashour, A. F., & Yang, K. H. (2008). Application of plasticity theory to reinforced concrete deep beams: A review. *Magazine of Concrete Research*, *60*(9), 657–664.

Bažant, Z. P., & Jirásek, M. (2002). Nonlocal integral formulations of plasticity and damage: Survey of progress. *Journal of Engineering Mechanics*, *128*(11), 1119–1149.

Bergmeister, K., Breen, J. E., Jirsa, J. O., & Kreger, M. E. (1993). *Detailing for structural concrete*. Austin, TX: Center for Transportation Research, University of Texas.

Biondini, F., Bontempi, F., & Malerba, P. G. (1999). Optimal strut-and-tie models in reinforced concrete structures. *Computer Assisted Mechanics and Engineering Sciences*, *6*(3–4), 280–293.

Bogomolny, M., & Amir, O. (2012). Conceptual design of reinforced concrete structures using topology optimization with elastoplastic material modeling. *International Journal for Numerical Methods in Engineering*, *90*, 1578–1597.

Bruggi, M. (2009). Generating strut-and-tie patterns for reinforced concrete structures using topology optimization. *Computers and Structures*, *87*(23–24), 1483–1495.

Bruggi, M. (2010). On the automatic generation of strut and tie patterns under multiple load cases with application to the aseismic design of concrete structures. *Advances in Structural Engineering*, *13*(6), 1167–1181.

Bruggi, M. (2016). A numerical method to generate optimal load paths in plain and reinforced concrete structures. *Computers and Structures*, *170*, 26–36.

Canadian Standards Association (CSA). (2004). *Design of concrete structures*. Rexdale, ON: Author.

Chou, Y.-H., & Lin, C.-Y. (2010). Improved image interpreting and modeling technique for automated structural optimization system. *Structural and Multidisciplinary Optimization*, *40*(1–6), 215–226.

Comite Euro-international du Beton. (1993). *CEB-FIP Model Code 1990 (Biulletind'information, no. 213/214)*. London: Author.

Du, Z., Zhang, W., Zhang, Y., Xue, R., & Guo, X. (2019). Structural topology optimization involving bi-modulus materials with

asymmetric properties in tension and compression. *Computational Mechanics*, *63*(2), 335–363.

El-Metwally, S., & Chen, W.-F. (2017). *Structural concrete: Strut-and-tie models for unified design*. Boca Raton, FL: CRC Press.

European Committee for Standardization (CEN). (2017). *Eurocode 2: Design of concrete structures-part 1-1: General rules and rules for buildings* (EN1992-1-1). Brussels: Author.

FIB. (2011). *Design examples for strut-and-tie models*. FIB Bulletin No. 61.

Gaynor, A. T., Guest, J. K., & Moen, C. D. (2013). Reinforced concrete force visualization and design using bilinear truss-continuum topology optimization. *Journal of Structural Engineering*, *139*(4), 607–618.

Guan, H. (2005). Strut-and-tie model of deep beams with web openings-an optimization approach. *Structural Engineering and Mechanics*, *19*(4), 361–380.

Guan, H., & Doh, J.-H. (2007). Development of strut-and-tie models in deep beams with web openings. *Advances in Structural Engineering*, *10*(6), 697–711.

Guest, J. K., Prévost, J. H., & Belytschko, T. (2004). Achieving minimum length scale in topology optimization using nodal design variables and projection functions. *International Journal for Numerical Methods in Engineering*, *61*(2), 238–254.

Guo, X., Zhang, W., & Zhong, W. (2014). Doing topology optimization explicitly and geometrically: A new moving morphable components based framework. *Journal of Applied Mechanics*, *81*(8), 081009.

Herranz, U. P., Maria, H. S., Gutierrez, S., & Riddell, R. (2012). Optimal strut-and-tie models using full homogenization optimization method. *ACI Structural Journal*, *109*(5), 605–614.

Hsu, M. H., & Hsu, Y. L. (2005). Interpreting three dimensional structural topology optimization results. *Computers and Structures*, *83*(4–5), 327–337.

Huang, H., Wu, S., Cohen-Or, D., Gong, M., Zhang, H., Li, G., & Chen, B. (2013). L1-medial skeleton of point cloud. *ACM Transactions on Graphics*, *32*(4), 61–65.

Huang, X., & Xie, Y. (2010). A further review of ESO type methods for topology optimization. *Structural and Multidisciplinary Optimization*, *41*(5), 671–683.

Jiang, W., Xu, K., Cheng, Z.-Q., Martin, R. R., & Dang, G. (2013). Curve skeleton extraction by coupled graph contraction and surface clustering. *Graphical Models*, *75*(3), 137–148.

Karthik, M. M., Mander, J. B., & Hurlebaus, S. (2016). Displacement-based compatibility strut-and-tie method and application to monotonic and cyclic loading. *Journal of Structural Engineering*, *142*(6), 4016010.

Kociecki, M., & Adeli, H. (2014). Two-phase genetic algorithm for topology optimization of free-form steel space-frame roof structures with complex curvatures. *Engineering Applications of Artificial Intelligence*, *32*, 218–227.

Kociecki, M., & Adeli, H. (2015). Shape optimization of free-form steel space-frame roof structures with complex geometries using evolutionary computing. *Engineering Applications of Artificial Intelligence*, *38*, 168–182.

Kwak, H. G., & Noh, S. H. (2006). Determination of strut-and-tie models using evolutionary structural optimization. *Engineering Structures*, *28*(10), 1440–1449.

Li, C., & Bovik, A. C. (2010). Content-weighted video quality assessment using a three-component image model. *Journal of Electronic Imaging*, *19*(1), 11003.

Li, Q. Q., Steven, G. P., & Xie, Y. M. (2006). On equivalence between stress criterion and stiffness criterion in evolutionary structural optimization. *Engineering Structures*, *28*(10), 1440–1449.

Liang, Q. Q., Xie, Y. M., & Steven, G. P. (2000). Topology optimization of strut-and-tie models in reinforced concrete structures using an evolutionary procedure. *ACI Structural Journal*, *97*(2), 322–332.

Liang, Q. Q., Xie, Y. M., & Steven, G. P. (2001). Generating optimal strut-and-tie models in prestressed concrete beams by performance-based optimization. *ACI Structural Journal*, *98*(2), 226–232.

Lin, C. Y., & Chao, L. S. (2000). Automated image interpretation for integrated topology and shape optimization. *Structural and Multidisciplinary Optimization*, *20*(2), 125–137.

Marti, P. (1985). Basic tools of reinforced concrete beam design. *ACI Journal Proceedings*, *82*(1), 46–56.

Mendoza-San-Agustin, A., Velázquez-Villegas, F., & ZepedaSánchez, A. (2016). Adaptation of topologic optimized structures based on skeletonization. *Ingeniería mecánica, tecnología y desarrollo*, *5*(4), 415–421.

Mezzina, M., Palmisano, F., & Raffaele, D. (2012). Designing simply supported RC bridge decks subjected to in-plane actions: Strut-and-tie model approach. *Journal of Earthquake Engineering*, *16*(4), 496–514.

Mörsch, E. (1909). *Concrete-steel construction (der eisenbetonbau)*. New York: McGraw-Hill.

Muttoni, A., Ruiz, M. F., & Niketic, F. (2015). Design versus assessment of concrete structures using stress fields and strut-and-tie models. *ACI Structural Journal*, *112*(5), 605–615.

Nana, A., Cuillière, J.-C., & Francois, V. (2017). Automatic reconstruction of beam structures from 3D topology optimization results. *Computers and Structures*, *189*, 62–82.

Nielsen, M. P. (1984). *Limit analysis and concrete plasticity*. Englewood Cliffs, NJ: Prentice Hall.

Paya, I., Yepes, V., González-Vidosa, F., & Hospitaler, A. (2008). Multiobjective optimization of concrete frames by simulated annealing. *Computer-Aided Civil and Infrastructure Engineering*, *23*(8), 596–610.

Perera, R., & Vique, J. (2009). Strut-and-tie modelling of reinforced concrete beams using genetic algorithms optimization. *Construction and Building Materials*, *23*(8), 2914–2925.

Reineck, K.-H. (2002). *Examples for the design of structural concrete with strut-and-tie mode*. Farmington Hills, MI: American Concrete Institute.

Ritter, W. (1899). Die bauweise hennebique. *Schweizerische Bauzeitung*, *33*(7), 59–61.

Schlaich, J., & Schafer, K. (1991). Design and detailing of structural concrete using strut-and-tie models. *Structural Engineer*, *69*(6), 113–125.

Schlaich, J., Schafer, K., & Jennewein, M. (1987). Toward a consistent design of structural concrete. *PCI Journal*, *32*(3), 74–150.

Sigmund, O., & Petersson, J. (1998). Numerical instabilities in topology optimization: A survey on procedures dealing with checkerboards, mesh-dependencies and local minima. *Structural Optimization*, *16*(1), 68–75.

Takezawa, A., Nishiwaki, S., & Kitamura, M. (2010). Shape and topology optimization based on the phase field method and sensitivity analysis. *Journal of Computational Physics*, *229*(7), 2697–2718.

Tan, K. H., Tong, K., & Tang, C. Y. (2001). Direct strut-and-tie model for prestressed deep beams. *Journal of Structural Engineering*, *127*(9), 1076–1084.

Tjhin, T. N., & Kuchma, D. A. (2007). Integrated analysis and design tool for the strut-and-tie method. *Engineering Structures*, *29*(11), 3042–3052.

van Dijk, N. P., Maute, K., Langelaar, M., & Van Keulen, F. (2013). Level-set methods for structural topology optimization: A review. *Structural and Multidisciplinary Optimization*, *48*(3), 437–472.

Victoria, M., Querin, O. M., & Marti, P. (2011). Generation of strut-and-tie models by topology design using different material properties in tension and compression. *Structural and Multidisciplinary Optimization*, *44*(2), 247–258.

Wang, Z., Bovik, A. C., Sheikh, H. R., & Simoncelli, E. P. (2004). Image quality assessment: From error visibility to structural similarity. *IEEE Transactions on Image Processing*, *13*(4), 600–612.

Yepes, V., Marti, J. V., & Garcia-Segura, T. (2015). Cost and CO_2 emission optimization of precast–prestressed concrete U-beam road bridges by a hybrid glowworm swarm algorithm. *Automation in Construction*, *49*, 123–134.

Yi, G., & Kim, N. H. (2017). Identifying boundaries of topology optimization results using basic parametric features. *Structural and Multidisciplinary Optimization*, *55*(5), 1641–1654.

Yi, G., Youn, B. D., & Kim, N. H. (2015). Geometric feature identification from topology optimization results. *11th World Congress on Structural and Multidisciplinary Optimisation*. Sydney, Australia.

Yu, M., Li, J., & Ma, G. (2009). *Theorems of limit analysis*. New York: Springer.

Zhang, T. Y., & Suen, C. Y. (1984). A fast parallel algorithm for thinning digital patterns. *Communications of the ACM*, *27*(3), 236–239.

Zhong, J. T., Wang, L., Deng, P., & Zhou, M. (2017). A new evaluation procedure for the strut-and-tie models of the disturbed regions of reinforced concrete structures. *Engineering Structures*, *148*, 660–672.

Zhou, L.-Y., He, Z.-Q., & Liu, Z. (2016). Investigation of optimal layout of ties in STM developed by topology optimization. *Structural Concrete*, *17*(2), 175–182.

How to cite this article: Xia Y, Langelaar M, Hendriks MAN. A critical evaluation of topology optimization results for strut-and-tie modeling of reinforced concrete. *Comput Aided Civ Inf*. 2020;35:850–869. https://doi.org/10.1111/mice.12537

APPENDIX

The principal stress plots of Case II and Case III are shown in the Figure A1 and Figure A2, where their extraction results are shown in Figure A3 and Figure A4.

The detailed settings of selected TO results are shown in Table A1. For the different mesh settings, the number indicates the ratio of coarse mesh size and refined mesh size.

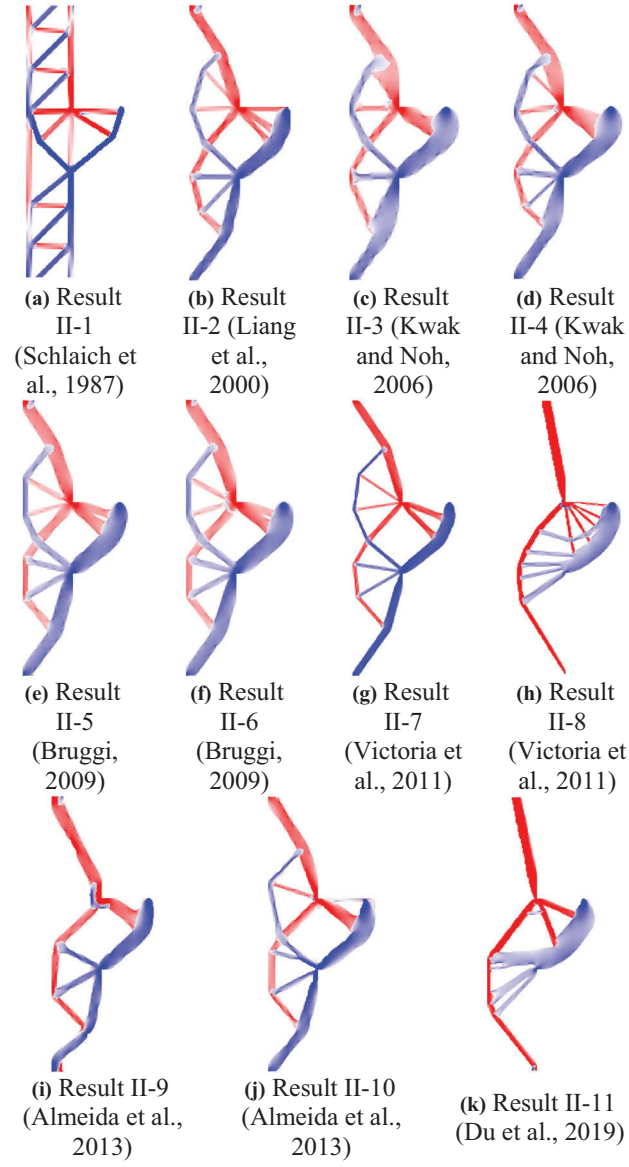

FIGURE A1 Principal stress plots of Case II: Corbel

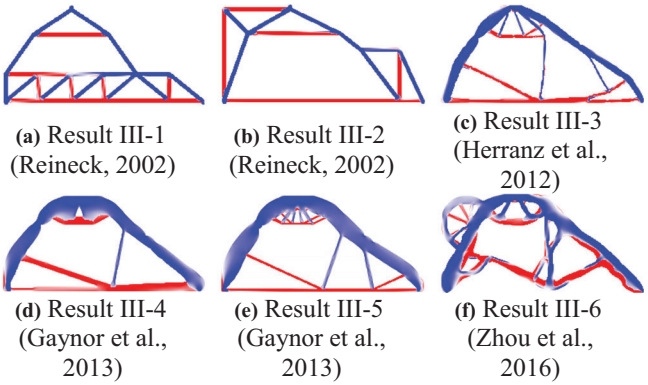

FIGURE A2 Principal stress plots of Case III: Dapped-end beam with opening

TABLE A1 Detailed information of selected TO results

Results	Literature	Method	Optimization setting	Special measure	Details
I-1	Schlaich et al. (1987)	STM (not based on TO)	–	–	–
I-2					
I-3	Liang et al. (2000)	ESO	Strain energy removal criterion	–	–
I-4	Kwak and Noh (2006)	ESO	Strain energy removal criterion	Micro-truss element	Coarse mesh
I-5					Refined mesh 1.5x
I-6	Victoria et al. (2011)	Isoline approach	Von Mises stress removal criterion	–	Volume fraction 17%
I-7				Different tensile and compressive modulus	Volume fraction 17%
I-8				–	Volume fraction 8%
I-9	Almeida et al. (2013)	Smooth ESO	Von Mises stress removal criterion	Smoothing constitutive relation	
I-10	This paper	SIMP	Minimizing compliance	–	Coarse mesh
I-11					Refined mesh 2x
II-1	Schlaich et al. (1987)	STM (not based on TO)	–	–	–
II-2	Liang et al. (2000)	ESO	Strain energy removal criterion	–	–
II-3	Kwak and Noh (2006)	ESO	Strain energy removal criterion	Micro-truss element	Coarse mesh
II-4					Refined mesh 1.5x
II-5	Bruggi (2009)	SIMP	Minimizing compliance	–	Coarse mesh
II-6					Refined mesh 4x
II-7	Victoria et al. (2011)	Isoline approach	Von Mises stress removal criterion	–	–
II-8				Different tensile and compressive modulus	–
II-9	Almeida et al. (2013)	Smooth ESO	Von Mises stress removal criterion	Smoothing constitutive relation	Coarse mesh
II-10					Refined mesh 4x
II-11	Du et al. (2019)	SIMP	Orthotropic constitutive relation	Different tensile and compressive modulus	–
III-1	Reineck (2002)	STM (not based on TO)	–	–	–
III-2					
III-3	Herranz et al. (2012)	Full-homogeneous method	Minimizing compliance	–	–
III-4	Gaynor et al. (2013)	Hybrid truss-continuum	Minimizing compliance	–	–
III-5				Different tensile and compressive modulus	
III-6	Zhou et al. (2016)	ESO	Axial stress removal criterion	Micro-truss elements	–

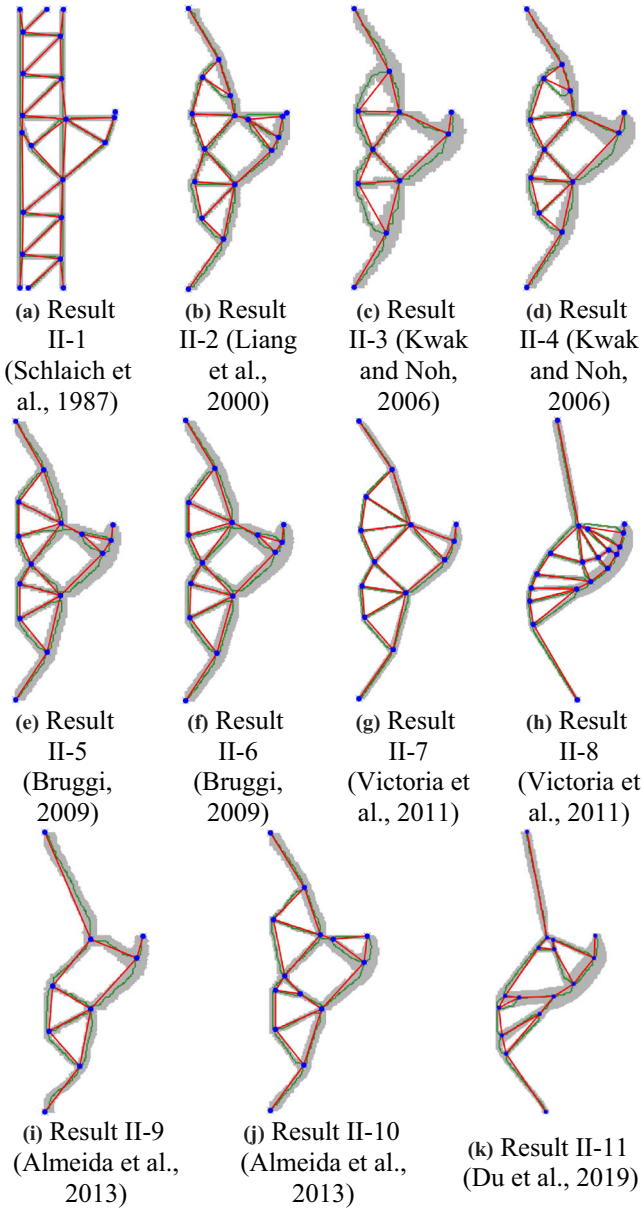

FIGURE A3 Extraction results of Case II: Corbel

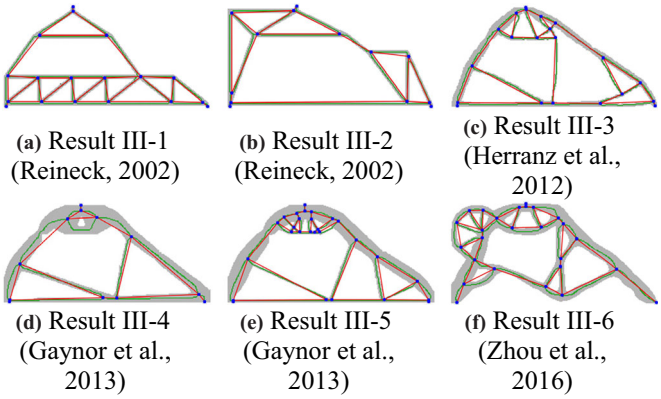

FIGURE A4 Extraction results of Case III: Dapped-end beam with opening